INSTITUTE OF PHYSICS PUBLISHING MEASUREMENT SCIENCE AND TECHNOLOGY
Meas. Sci. Technol. **14** (2003) 2027–2033 PII: S0957-0233(03)62926-7

A novel application of speckle interferometry for the measurement of strain distributions in semi-sweet biscuits

Q Saleem[1], **R D Wildman**[1], **J M Huntley**[1] **and M B Whitworth**[2]

[1] Wolfson School of Mechanical and Manufacturing Engineering, Loughborough University, LE11 3TU, UK
[2] Campden & Chorleywood Food Research Association, Chipping Campden GL55 6LD, UK

Received 28 April 2003, in final form 29 July 2003, accepted for publication 29 August 2003
Published 2 October 2003
Online at stacks.iop.org/MST/14/2027

Abstract
The spontaneous formation of cracks in biscuits following baking, also known as checking, is an issue that manufacturers would like to be able to predict and avoid. Unfortunately the mechanisms driving this phenomenon are not well understood. Speckle interferometry was used to study moisture-induced in-plane strain development in biscuits. This sensitive and non-contacting technique for measuring surface displacements has two major advantages over more commonly used methods; firstly, strains can be detected at a far higher sensitivity (down to 2×10^{-6}) than previously accessible and secondly the method is a whole-field technique, enabling observation of the development of strain distributions during moisture migration. For biscuits exposed to step changes in humidity, initial strain rates of up to 10^{-5} min^{-1} were measured, which decreased as the moisture content approached equilibrium, leading to an accumulated strain of $\sim 10^{-2}$ after 48 h. Under these conditions, a homogeneous, uniform strain distribution was observed. The data were used to calculate the hygroscopic expansion coefficient, which was linearly related to moisture content and provides the necessary constitutive link between strain and biscuit moisture content needed to model biscuit checking.

Keywords: biscuit checking, semi-sweet biscuits, moisture migration, moisture-induced strain, speckle interferometry, non-contacting technique, whole-field measurements, hygroscopic expansion coefficient

1. Introduction

Biscuits with reduced fat content have shown a tendency to crack up to several hours after the baking process in a phenomenon that has become known as biscuit checking. The crack development makes the biscuit weak, making it more susceptible to breakage under the application of small loads. It has been suggested [1–3] that the central and thicker parts of the biscuit have slightly higher moisture contents than edge regions after the drying process in the baking oven. When the biscuit cools down, moisture diffuses from regions of high moisture content (the centre) to areas with less moisture (the edges). This moisture migration leads to expansion towards the edge of the biscuit and contraction at the centre, causing stresses to build up in the biscuit. When these stresses exceed the structural strength of the biscuit, cracks develop. This is highly undesirable and a phenomenon that biscuit manufacturers wish to avoid. Historically, however, there has been little scientific research into the processes involved during checking, leaving the problem poorly understood and the biscuit manufacturers disadvantaged as consumers change brand loyalty due to dissatisfaction with the product [2].

Previous attempts to produce reduced fat biscuits have highlighted the tendency that certain types of biscuits are more susceptible to checking than others [4]. The features that have been associated with biscuit checking are a fat to flour ratio of

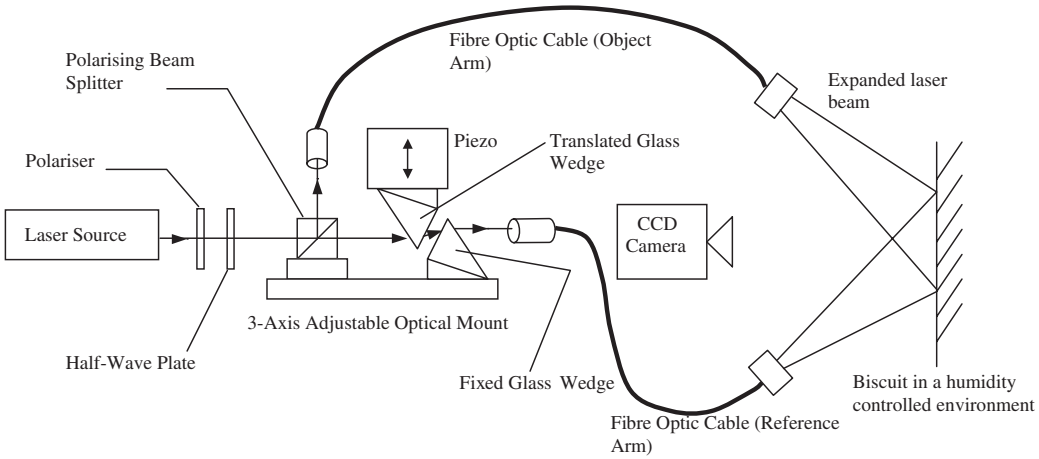

Figure 1. Layout of components in the speckle interferometry system for experiments on semi-sweet biscuits.

15:100 or less in addition to low sugar content and a denser, less aerated texture. Conversely, an increased fat content and more aerated texture tends to make biscuits more flexible and less brittle, leading to a reduced likelihood of checking. In the light of recent nutritional advice to reduce the amount of fat eaten in the diet, manufacturers are keen to resolve these issues although, until now, such attempts have been somewhat empirical.

A problem faced by those attempting to address the biscuit checking problem is the lack of a standard method for testing or predicting checking. Moreover, traditional methods of measuring strain have been difficult to apply to biscuits because of the nature of food materials, the small magnitude of the strains and the difficulty of attaching gauges to the product. The scarcity of research in this field highlights the need for whole-field, high accuracy strain measurements, as supplied by optical techniques such as speckle interferometry. The coupling of these experiments with numerical methods, such as finite element modelling (FEM), provides the potential for major advances in this area.

In this paper a method for examining strain fields in biscuit materials is presented. The paper is divided into two main sections. In section 2, speckle interferometry is introduced in the context of measuring displacement fields in food materials and the experimental apparatus is described. This is followed by a description of the data analysis methods needed to produce strain fields. In section 3 the usefulness and limitations of the technique are discussed with reference to experiments on biscuit materials, and measurements of the hygroscopic expansion coefficient are presented.

2. Experimental approach

2.1. Experimental methodology for biscuit materials

Optical interference is a widely known phenomenon that is due to the superposition of two beams of light, leading to an enhancement (constructive) or a reduction (destructive) in the amplitude of the rays. Although most sensors are sensitive to intensity rather than amplitude and phase, interferometry is a subject that concerns itself with phase differences and, by implication, path differences [5–11]. These phase differences are typically generated from coherent sources of light such as lasers, and the resulting variation in intensity is detected by devices such as CCD (charge coupled device) cameras. The developments of classical interferometry include holography, moiré and speckle techniques and are used in a wide range of industrial applications [12].

Speckle interferometry is a particularly useful method for observing the behaviour of rough surfaces such as biscuits, as it relies on the variation of the specimen surface to produce the distinctive speckle patterns [5, 12]. Changes in the observed speckle pattern can be correlated with deformation of the material and used to measure the displacements and strains at its surface. There are several strengths of this technique that make it highly suitable for measuring displacement and strain distributions in biscuits. First of all, the method is non-contacting and does not require modification of the specimen, such as the preparation of a grating on the specimen surface as in grid [13–17] and moiré [18–22] techniques. It therefore enables determination of the required displacement and strain information without any physical contact with the sample or reinforcement of it—a big advantage when studying biscuits, which are delicate and difficult to handle. Second, strains can be detected at a far higher sensitivity (down to 2×10^{-6}) than previously accessible, and third the method is a whole-field technique, potentially enabling observation of the development of strain distributions during moisture migration. The combination of these improvements over traditional strain measurement methods makes speckle interferometry an ideal method for studying biscuit checking.

2.2. Speckle interferometry

A phase-shifting digital speckle interferometer was constructed to measure the moisture-dependent biscuit surface displacements and is shown in schematic form in figure 1. A 10 mW He–Ne laser beam (wavelength $\lambda = 632.8$ nm) was used as a source of illumination. The beam was vertically polarized and split into two beams using a polarizing beam-splitter. One beam was passed through a piezo-controlled glass wedge to enable small path differences to be introduced in a controlled fashion. The resultant beams were then used to illuminate the specimen area of interest. The angle between

beams at the biscuit surface was 61.52°. The reflected light from the biscuit was collected onto a CCD array positioned normal to the biscuit surface. The camera used was a Kodak ES 1.0 digital CCD device, which has a maximum framing rate of 30 frames s^{-1} and a resolution of 1024 × 1024 pixels. A path difference introduced into the two beams results, due to the surface microstructure, in a complex interference pattern that reflects the topology of the biscuit. A straining of the surface results in the path and phase differences being altered and produces a modified interference pattern. This technique therefore allows measurement of the phase changes due to the deformation of the surface in relation to the reference state.

The primary parameter of interest during speckle interferometry experimentation is the measurement of phase, which can be determined uniquely by phase shifting. This is a process in which known phase shifts are introduced between the two interfering beams, enabling the phase to be extracted by measuring the fringe or speckle intensity. The phase shift (or modulation) can be either a function of time or of position in the image. In the former case the resulting intensity distributions are sampled at discrete time intervals and the method is known as temporal phase shifting; in the latter case, a single intensity distribution is sampled at discrete points in the image, in which case it is referred to as spatial phase shifting. In the interferometer constructed for the measurement of strains in biscuits, temporal phase shifting was employed. The phase shifting was achieved by a glass wedge placed in one of the two beams and pushed by a piezoelectric translator (PZT) [12].

A range of phase shifting algorithms has been suggested in the literature [23–26]. Early versions were constructed purely to allow the unique determination of the phase distribution, but recent advances have been made in reducing both systematic and mis-calibration errors by extending the number of frames collected from 4 or 5 to 10, 15 or more [5]. Although this does suppress the propagation of errors through the analysis, it takes a proportionally larger time to capture and analyse one set of frames. Analysis of the results of 5 and 10 frame algorithms showed no significant improvement for 10 frames and therefore the more rapid algorithm using 5 frames [27] was chosen for the analysis.

2.3. Fringe analysis

The production of strain fields involves a number of steps, including the development of phase maps, phase unwrapping and strain field extraction.

2.3.1. Calculation of phase maps. The interferograms obtained from the speckle interferometer through phase shifting were analysed by a fringe analysis program, which can be used interactively or for off-line analysis. The latter option is very useful for repeated processing of fringe patterns obtained under similar conditions and was used for the present work. The instructions required for fringe analysis are stored in a control file. The program, as per instructions specified in the control file, then carries out each operation. The first task performed by the fringe analysis program was the calculation of wrapped phase maps. In the wrapped phase maps, it is very important to minimize the influence of noise, including speckle noise. One particularly successful method of achieving noise reduction is to filter the data using a convolution kernel following the method (spatial speckle averaging) described in [5]. This involves smoothing the cosine and sine images of the phase change by replacing the value at each pixel by the local average calculated over a 3 × 3 pixel filter size. The convolution process makes the images smooth but very large filter sizes may result in the loss of experimental data.

2.3.2. Calculation of phase change and phase unwrapping. The phase change distribution is calculated relative to some initial reference interferogram, which in the present case corresponds to the undeformed state of the specimen. The calculated phase change values lie in the range $(-\pi, \pi)$; phases outside this range are wrapped. Phase unwrapping is a process by which the absolute value of the phase change of a continuous function that extends over a range of more than 2π (relative to a predefined starting point) is recovered. This absolute value is lost when the phase term is wrapped upon itself with a repeat distance of 2π due to the fundamental sinusoidal nature of the wavefunctions used in the measurement of physical properties. Phase unwrapping is a process of adding correct integral multiples of 2π to each pixel's phase value. It is used to remove the 2π phase discontinuities and the removal can be carried out either along the time axis or spatially, known respectively as temporal and spatial unwrapping. In the present work spatial unwrapping was used because temporal unwrapping requires experimentation at fast sampling intervals (a few seconds), which results in very large numbers of images to be processed. As experiments on biscuit materials were conducted over periods of up to 48 h, it would have been impractical to handle and process the amount of data yielded by temporal unwrapping.

The key to reliable phase unwrapping algorithms is the ability to detect the 2π phase jumps accurately. In the case of phase data that are noise-free and adequately sampled (i.e. the true phase changes lie in the range of 2π), a simple approach to phase unwrapping is adequate and it suffices to make a sequential scan through the data (line by line) to integrate the phase by adding or subtracting 2π at the phase jumps. In many measurement situations, noise in the sampled data is responsible for the false identification of phase jumps and to cope with this problem many sophisticated phase unwrapping algorithms have been developed. One of the most successful classes of unwrapping algorithms is the so-called 'branch-cut' method [27–29]. In the present work we use the branch-cut algorithm developed in [28].

2.3.3. Strain field extraction. Once the unwrapped phase maps have been obtained the displacement field is calculated by multiplying the phase data by the scaling factor ($c = \lambda/4\pi \sin\theta$), which in this case takes the value $c = 0.0985\ \mu\text{m rad}^{-1}$. Strain fields were calculated through a process of numerical differentiation. This was achieved by fitting a plane through a square region (with a dimension known as the gauge length or filter size) and calculating strains from the gradients. The effect of gauge length on the noise in the final strain maps was studied by using four different gauge lengths: 25 × 25, 37 × 37, 49 × 49 and 61 × 61 pixels. The use of higher gauge lengths resulted in lower standard deviation values for strain, which implies lower noise in the

Table 1. Dough composition for semi-sweet biscuits used in speckle interferometry experimental work.

Ingredient	% flour (by weight)
Flour	100
Fat	12
Sugar (pulverized)	20.83
Glucose	1.31
Salt	1.20
Sodium bicarbonate	0.50
Ammonium bicarbonate	1.07
Water	22.80
Sodium acid pyrophosphate	0.19
Sodium metabisulfite	0.02

Table 2. Saturated salt solutions and their equilibrium relative humidity values at the given temperatures used for experiments on semi-sweet biscuits.

Salt solution	Temperature (°C)	Equilibrium relative humidity (%)
Lithium chloride (LiCl)	20.8	17.0
Potassium acetate (CH_3COOK)	21.0	28.8
Magnesium chloride ($MgCl_2$)	21.1	39.5
Potassium carbonate (K_2CO_3)	20.5	51.0
Sodium dichromate ($Na_2Cr_2O_7$)	20.6	60.5
Ammonium nitrate (NH_4NO_3)	20.6	70.1
Sodium chloride (NaCl)	20.7	80.2
Potassium chloride (KCl)	20.1	90.8

strain maps and suggested that higher gauge lengths should be used. However, it must be noted that the use of a higher gauge length requires more time for calculation of strains from displacement. This factor is even more important when the number of images is very large, as in the case of biscuit materials. Therefore as a compromise between the gauge length and the solution time a gauge length of 49×49 pixels was used to process all the data, corresponding to a physical gauge length on the specimen of 5.74×5.74 mm^2.

2.4. Validation of speckle interferometer

An important element in constructing the speckle interferometer was its calibration and validation. This was done by comparing the measured rotation of an aluminium block using a micrometer rotation stage and the speckle interferometer. A series of rotations were applied in increments of $1/12°$, as determined using the micrometer. The displacement of the block for each rotation angle was then measured using the optical procedure detailed in sections 2.2 and 2.3. The displacement was measured as a function of position and the applied rotation was estimated by linear regression against the experimental data. Comparison of the actual rotation and the measured value showed a difference of less than 1%, indicating the accuracy with which displacement and strain fields can be measured.

2.5. Preparation of biscuits

The biscuits used in this study were baked on a pilot scale at Campden and Chorleywood Food Research Association (Chipping Campden, UK). The dough composition used to produce semi-sweet biscuits is given in table 1. Doughs were mixed in a Z-blade mixer, sheeted to a thickness of 1.3 mm, cut to shape and baked in a travelling oven for $2\frac{1}{4}$ min at 149 °C and a further $2\frac{1}{4}$ min at 227 °C.

3. Results and discussion

The main experimental work was focused on the measurement of displacement and strain distributions for biscuits subjected to step changes in external humidity over a range of 17–91% and strains were calculated from the displacement gradients. The displacement measurements were made at sampling intervals increasing from 2 to 90 min because of the reduced expansion of the biscuit sample with time. The duration of the experiments varied from 20 to 48 h for different humidity step changes. The humidity was controlled by placing the biscuits in a sealed container together with saturated salt solutions of differing equilibrium relative humidity. A list of solutions used is given in table 2. Prior to strain measurements, the biscuits were initially conditioned in plastic boxes with dishes of the required saturated salt solution for 48 h to reach equilibrium. They were transferred to an environment of higher humidity in a humidity chamber fitted with a transparent glass lid, through which speckle interferometry measurements could be made. A fan was used to maintain a uniform humidity within the chamber, but was turned off to minimize vibration during acquisition of speckle patterns. The increase in humidity led to an increase in the moisture content of the biscuits. The resulting dilation was measured with the speckle interferometer. The room temperature during the speckle interferometry experiment was observed to be constant to within 1 °C (20 ± 1 °C). The initial images obtained from the speckle interferometer were processed as per section 2.3.1 to obtain wrapped phase maps. A sequence of wrapped phase maps during a 51–60.5% humidity step change is shown in figure 2. Each map corresponds to the displacement over a time interval of 12 min. These wrapped phase maps show a decrease in the number of fringes with time, corresponding to a decrease in the expansion rate of the sample. The wrapped phase maps involve 2π discontinuities and were therefore unwrapped as per section 2.3.2, prior to calculation of the displacement and strain information. The corresponding unwrapped phase maps are shown in figure 3.

3.1. Displacement and strain fields

The unwrapped phase maps give true phase change values, which are directly proportional to displacement values [8]. The strain values were then calculated as per section 2.3.3. The average strain as a function of time for the 60.5–70.1% humidity step change is shown in figure 4. It is evident from the figure that the biscuit showed a rapid initial strain rate and a lower rate at longer times.

The displacement and strain maps for the x component obtained for a 17–28.8% step change in humidity are shown in figure 5. These were the cumulative results obtained after 20 h. The displacement map shows that the maximum displacement occurred at the outer edges, each of which moved 60 μm during the specified humidity step change, corresponding to a total expansion in diameter of approximately 120 μm. It can

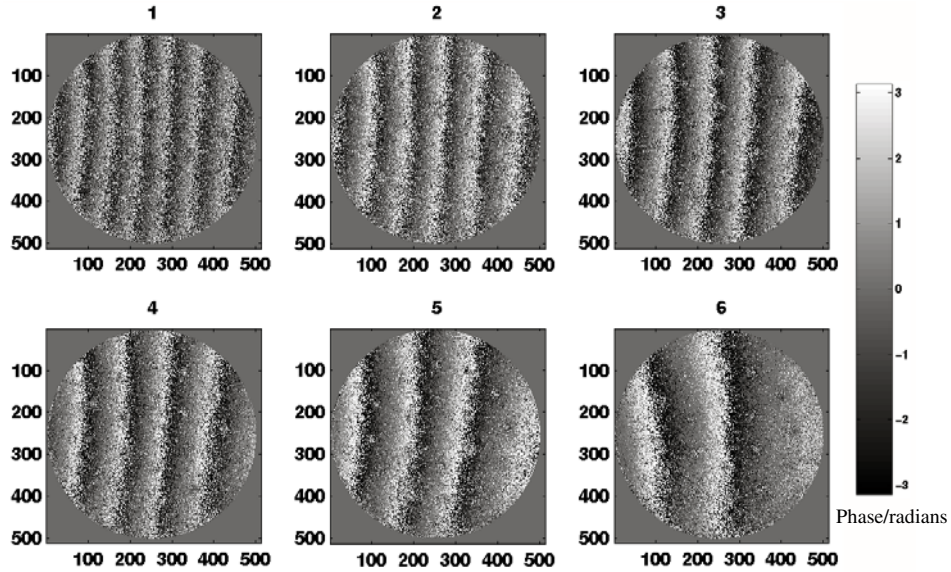

Figure 2. Incremental wrapped phase maps during a 51–60.5% humidity step change for semi-sweet biscuits (x and y axes showing the number of pixels).

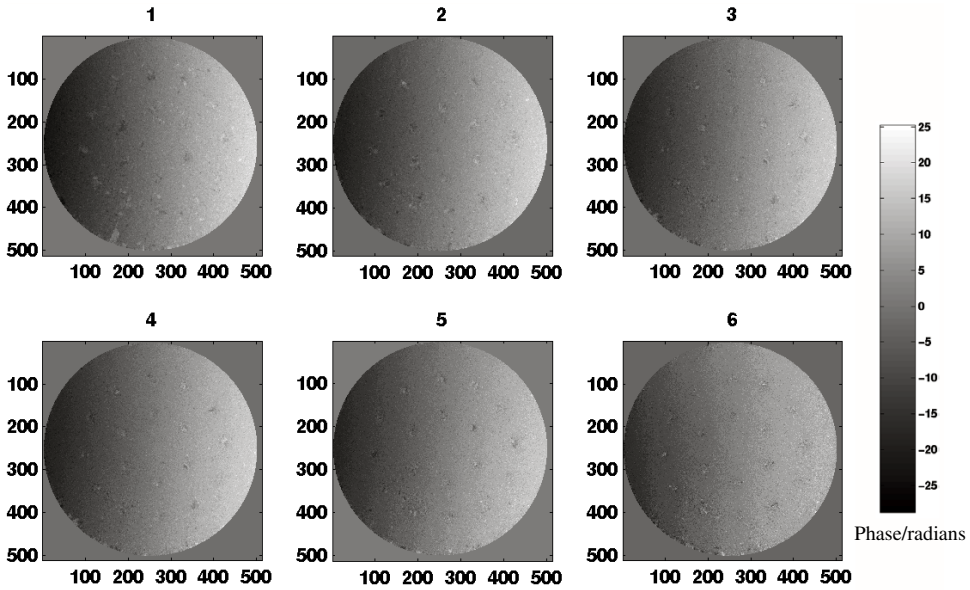

Figure 3. Incremental unwrapped phase maps during a 51–60.5% humidity step change for semi-sweet biscuits, calculated from figure 2 (x and y axes showing the number of pixels).

also be seen that the displacement distribution was quite uniform for the given step change in humidity. The strain map (figure 5(b)) also showed a homogeneous, uniform strain distribution. Figure 6 shows similar results for a step change of 60.5–70.1%. As exemplified by these results, it was found that step changes at high humidities gave greater displacement and strain values than comparable changes at lower humidities (figure 6).

3.2. Estimation of random error in average strain

The average strains were calculated from strain maps as well as from the displacement maps. A central region of the same size as the gauge length (i.e. 49×49 pixels) was chosen in the displacement map. From each row the strain was calculated as a slope by fitting a straight line through all the elements of that row. The average strain was then calculated by averaging all the strain values obtained from different rows of the chosen region. A measure of the error was then calculated from the standard deviation of the strains about the mean. The random error in calculated strains was estimated as 1% of the total strain.

3.3. Determination of hygroscopic expansion coefficient

The hygroscopic expansion coefficient is a measure of the expansion caused by a unit increase in moisture content of the sample. The moisture content for biscuits equilibrated to each of the chosen humidity levels was measured by an oven drying method (crushing and measuring

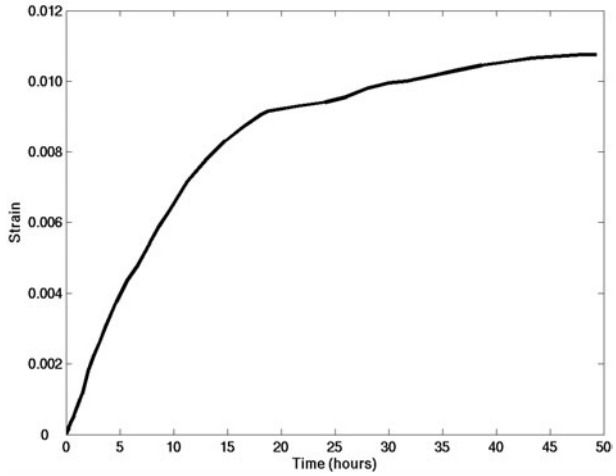

Figure 4. Average strain as a function of time for a 60.5–70.1% humidity step change.

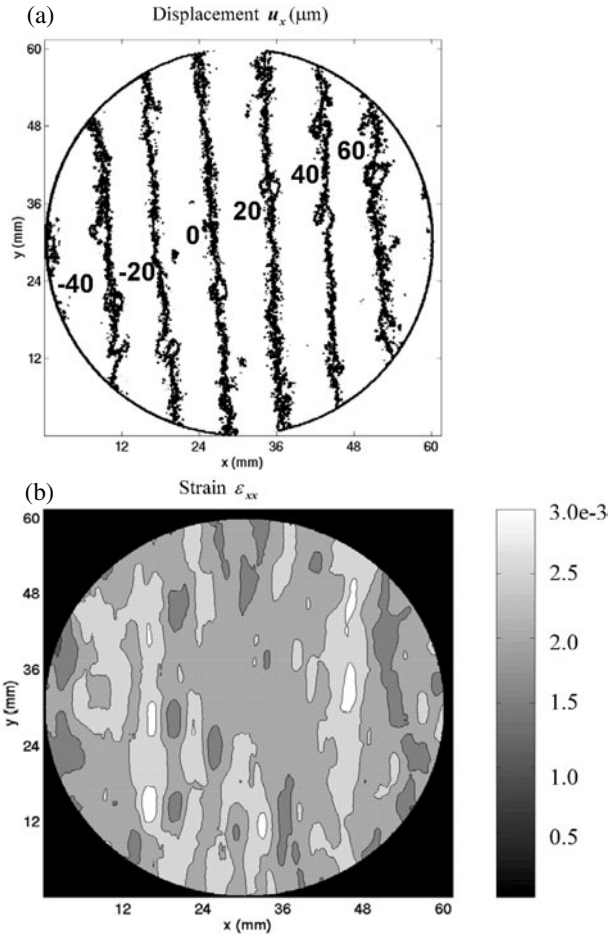

Figure 5. Cumulative displacement (a) and strain (b) maps after 20 h resulting from a 17–28.8% humidity step change for semi-sweet biscuits.

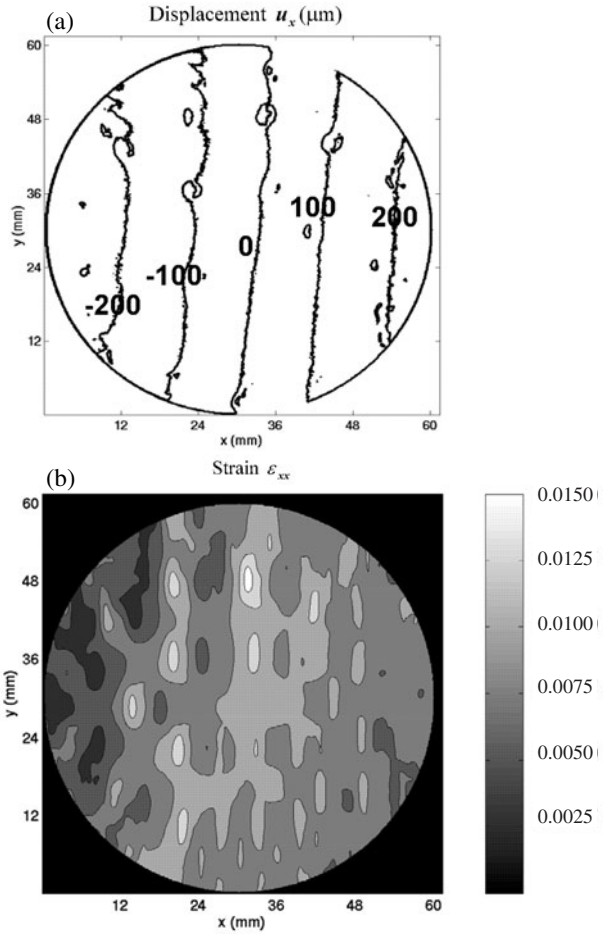

Figure 6. Cumulative displacement (a) and strain (b) maps after 44 h resulting from a 60.5–70.1% humidity step change for semi-sweet biscuits.

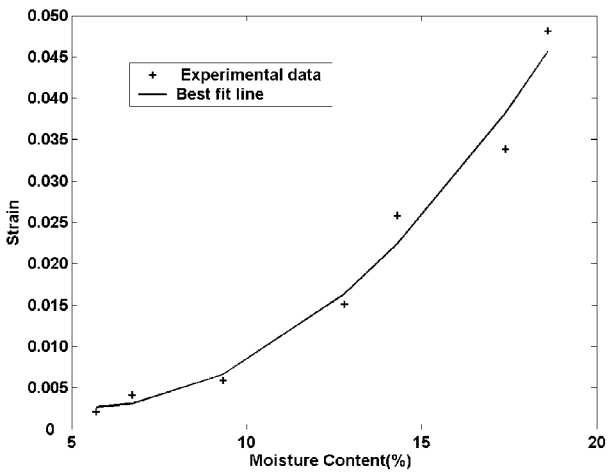

Figure 7. Average strain as a function of biscuit moisture content with second-order fit.

the change in mass after drying for 90 min at 130 °C). A non-linear dependence of measured strain on moisture content was observed from the speckle interferometry experiments on semi-sweet biscuits as shown in figure 7. A second-order polynomial was fitted to the experimental data points to extract the hygroscopic expansion coefficient (strain = 0.0005*(moisture)^2 − 0.005*(moisture) + 0.0181 and gradient = 0.001*(moisture) − 0.005). The slope of the fitted curve is the apparent hygroscopic expansion coefficient of the biscuits. There have been few previously reported

measurements of the hygroscopic expansion coefficient of biscuits. The hygroscopic expansion coefficient of crackers has been measured by direct measurements of the changes in the distances between points on the cracker surface for moisture contents of 1.5–4.5% [3]. The hygroscopic expansion coefficient values measured for semi-sweet biscuits in this study are in agreement with those obtained for crackers. However, there are two novel aspects of the present study for the determination of the hygroscopic expansion coefficient. Firstly, by using electronic speckle pattern interferometry (ESPI) for the measurements, it was possible to verify the uniformity of the strain field used for determination of the hygroscopic expansion coefficient. This technique also has greater versatility, enabling it also to be applied to the measurement of non-uniform strain fields such as those that may occur in freshly baked biscuits prior to checking. Secondly, the hygroscopic expansion coefficient has been determined as a function of biscuit moisture content over a wider moisture content range. These data can be used to carry out a materially non-linear stress analysis for a given moisture distribution in the biscuit.

4. Conclusions

Speckle pattern interferometry has been used for the measurement of strain distributions in semi-sweet biscuits. The measurements made using the proposed method are the most sensitive and the first whole-field measurements yet made of strains in biscuits. Knowledge of the hygroscopic expansion coefficient obtained from these measurements is an important prerequisite for quantitative modelling and understanding of the biscuit checking phenomenon. Speckle interferometry was found to be an ideal method for the measurement of strain distributions in biscuits as it is a very sensitive and non-contacting technique for measuring surface displacements and strains. For biscuits exposed to step changes in humidity, initial strain rates of up to $10^{-5}\,\mathrm{min}^{-1}$ were measured, which decreased as the moisture content approached equilibrium, leading to an accumulated strain of $\sim 10^{-2}$ after 48 h. Under these conditions, a homogeneous, isotropic strain distribution was observed. The data were used to calculate the hygroscopic expansion coefficient, which was linearly related to moisture content. The hygroscopic expansion coefficient results will be combined with measurements of other important biscuit properties, such as the moisture diffusion coefficient, Young's modulus and failure stress and strain. This will quantify the constitutive relations governing the behaviour of biscuits and enable the construction of a model of the biscuit checking phenomenon. The model will be validated by measurements of strains in biscuits during checking, making use of the optical technique described above.

References

[1] Dunn J A and Bailey C H 1928 Factors influencing checking in biscuits *Cereal Chem.* **5** 395–430

[2] Williams Y A and Wrigley C W 1995 *Cereals 95, Proc. 45th Australian Cereal Chemistry Conf. (Adelaide, South Australia)* (Melbourne: Royal Australian Chemical Institute) pp 299–302

[3] Kim M H and Okos M R 1999 Some physical, mechanical, and transport properties of crackers related to the checking phenomenon *J. Food Eng.* **40** 189–98

[4] Anon 1998 Cool running (cooling and handling) *Biscuit World* 16–8

[5] Huntley J M 1998 Automated fringe pattern analysis in experimental mechanics: a review *J. Strain Anal.* **33** 105–25

[6] Huntley J M, Melin L G, Goldrein H T, Nilsson S and Palmer S J P 1998 A study of mode-I delamination cracks by high-magnification moiré interferometry *Comput. Sci. Technol.* **58** 515–25

[7] Jones R and Wykes C 1989 *Holographic and Speckle Interferometry* (Cambridge: Cambridge University Press)

[8] Sirohi R S 1993 *Speckle Metrology* (New York: Dekker)

[9] Erf R K 1978 *Speckle Metrology* (New York: Academic)

[10] Dainty J C and Ennos A E 1984 Speckle interferometry *Laser Speckle and Related Phenomena* (Berlin: Springer) pp 203–54

[11] Moore A J and Tyrer J R 1995 Phase stepped ESPI and moiré interferometry for measuring stress intensity factor and J-integral *Exp. Mech.* **35** 306–14

[12] Robinson D W and Reid G T 1993 *Interferogram Analysis* (Bristol: Institute of Physics Publishing)

[13] Haynes A R and Coates P D 1996 Semi-automated image analysis of the true tensile drawing behaviour of polymers to large strains *J. Mater. Sci.* **31** 1843–55

[14] Huntley J M, Goldrein H T and Palmer S J P 1995 Automated fine grid technique for measurement of large-strain deformation maps *Opt. Lasers Eng.* **23** 305–18

[15] Sadat A B and Reddy M Y 1989 Plastic strain analysis of the machined surface region using fine grid etched by photoresist technique *Exp. Mech.* **29** 346–9

[16] Parks V J 1982 Strain measurement using grids *Opt. Eng.* **21** 633–9

[17] Carolan R, Egashira M, Kishimoto S and Shinya N 1992 The effect of grain boundary deformation on the creep micro-deformation of copper *Acta Metall. Mater.* **40** 1629–36

[18] Post D 1991 Moiré interferometry: advances and applications *Exp. Mech.* **31** 276–80

[19] Parks V J 1987 *Geometric Moiré Handbook on Experimental Mechanics* ed A S Kobayashi (Englewood Cliffs, NJ: Prentice-Hall) pp 282–313

[20] McDonach A, McKelvie J and Walker C A 1980 Stress analysis of fibrous composites using Moiré interferometry *Opt. Lasers Eng.* **1** 85–105

[21] Kobayashi A S (ed) 1993 *Handbook on Experimental Mechanics* (Bethel, CT: Society for Experimental Mechanics)

[22] Theocaris P S 1969 *Moiré Fringes in Strain Analysis* (Elmsford, NY: Pergamon)

[23] Surrel Y 1997 Additive noise effecting digital phase detection *Appl. Opt.* **36** 271–6

[24] Larkin K G and Oreb B F 1992 Design and assessment of symmetrical phase shifting algorithms: a-optics image science and vision *J. Opt. Soc. Am.* A **9** 1740–8

[25] Surrel Y 1996 Design of algorithms for phase measurements by the use of phase stepping *Appl. Opt.* **35** 51–60

[26] Schiwder J, Burow R, Essner K E, Grzanna J, Spolaczyk R and Merkel K 1983 Digital wave front measuring interferometry: some systematic error sources *Appl. Opt.* **22** 3421–32

[27] Huntley J M 2000 Automated analysis of speckle interferograms *Digital Speckle Pattern Interferometry and Related Techniques* ed P K Rastogi (Chichester: Wiley) pp 59–139

[28] Cusack R, Huntley J M and Goldrein H T 1995 Improved noise immune phase unwrapping algorithm *Appl. Opt.* **34** 781–9

[29] Huntley J M 1989 Noise immune phase unwrapping algorithm *Appl. Opt.* **28** 3268–70